Combining national forest inventories reveals distinct role of climate on tree recruitment in European forests

Louis A. König [a,b,c,*], Frits Mohren [b], Mart-Jan Schelhaas [a], Julen Astigarraga [d], Emil Cienciala [e,f], Roman Flury [g], Jonas Fridman [h], Leen Govaere [i], Aleksi Lehtonen [j], Adriane E. Muelbert [k], Thomas A.M. Pugh [k,l,m], Brigitte Rohner [g], Paloma Ruiz-Benito [d,n], Susanne Suvanto [j,k], Andrzej Talarczyk [o], Miguel A. Zavala [d], Jose Medina Vega [p], Igor Staritsky [a], Geerten Hengeveld [q], Gert-Jan Nabuurs [a,b]

[a] Wageningen Environmental Research (WENR), Wageningen University and Research, Droevendaalsesteeg 3, 6708 PB, Wageningen, The Netherlands.
[b] Forest Ecology and Management Group, Wageningen University, Droevendaalsesteeg 3, 6708 PB, Wageningen, The Netherlands
[c] Forest Ecology, ETH Zurich, Universitätsstrasse 16, 8092 Zürich, Switzerland
[d] Universidad de Alcalá, Forest Ecology & Restoration Group (FORECO), Departamento de Ciencias de la Vida, 28805 Alcalá de Henares, Madrid, Spain
[e] IFER - Institute of Forest Ecosystem Research, Cs. Armady 655, 254 01 Jilove u Prahy, Czech Republic
[f] Global Change Research Institute of the Czech Academy of Sciences, Belidla 986/4, 603 00 Brno, Czech Republic
[g] Swiss Federal Institute for Forest, Snow and Landscape Research WSL, Forest Resources and Management, Zürcherstrasse 111, CH-8903 Birmensdorf, Switzerland
[h] Swedish University of Agricultural Sciences, Department of Forest Resource Management, SE-90183 Umeå, Sweden
[i] Agency for Nature and Forests, Herman Teirlinck, Havenlaan 88 bus 75, 1000 Brussel, Belgium
[j] Natural Resources Insitute Finland, Latokartanonkaari 9, 00790, Helsinki, Finland
[k] School of Geography, Earth and Environmental Sciences, University of Birmingham, UK
[l] Department of Physical Geography and Ecosystem Science, Lund University, Sölvegatan 12, 22362 Lund, Sweden
[m] Birmingham Institute of Forest Research, University of Birmingham, Edgbaston, Birmingham, B15 2TT, UK
[n] Universidad de Alcalá, Grupo de Investigación en Teledetección Ambiental (GITA), Departamento de Geología, Geografía y Medio Ambiente, 28801 Alcalá de Henares, Madrid, Spain
[o] Forest and Natural Resources Research Centre Foundation, ul. Płomyka 56A, 02-491 Warszawa, Poland
[p] Forest Global Earth Observatory, Smithsonian Tropical Research Institute, Washington, DC, USA
[q] Biometris, Wageningen University and Research, Droevendaalsesteeg 3, 6708PB, Wageningen, The Netherlands

ARTICLE INFO

ABSTRACT

Tree recruitment forms an essential process in forest growth models as it determines the amount and composition of the next generation of trees and, hence, the provision of forest ecosystem services over long time spans. With global change and the hereby associated changes in environmental conditions and forest management adaptations, the common static tree recruitment modelling approaches have become largely obsolete and necessitated the development of more dynamic models. Limited by the availability of data for the parameterisation of tree recruitment processes, such models have only been developed for single species or national frameworks and largely failed to detect climatic influences. In this study, we developed a dynamic tree recruitment model for Europe, utilising National Forest Inventory data from 8 countries with more than 95,000 repeated plot observations and nearly 138,000 individual tree recruitment events. We investigated the effect of forest management, forest structure, soil characteristics, nutrient deposition and five groups of weather and climate variables on the quantity and the species composition of recruiting trees. The climatic groups spanned annual averages, intra annual averages, annual variability, intra annual extremes and a combination of the aforementioned groups. The model with the combination of climate and weather variables outperformed all other groups. We found distinct climatic effects on tree recruitment quantities linked to water limitations and temperature extremes. The results as such showed that tree recruitment quantities benefit from stable climatic conditions, high precipitation and suffer from high maximum temperatures. Increasing temperatures also facilitate the share of recruiting broadleaves. The recruitment species was largely determined by the lead species in a plot, indicating the importance of seed limitation. Furthermore, the results confirm the important role of forest structure in tree recruitment and

---

enable forest managers to steer the next generation of trees. Especially multi-species stands show a clear advantage over single species stands regarding tree recruitment quantities and diverse species compositions. Our research enables dynamic and state-of-the-art recruitment simulations across forests in Europe. It presents a reproducible method that can be applied to forest simulation modelling frameworks.

1. Introduction

Models of forest dynamics are essential tools to describe, understand and predict forest dynamics under climate change and alternative management strategies (Weiskittel et al., 2011; Vanclay, 2014; Bugmann and Seidl, 2022). In modelling forest dynamics, key population processes are recruitment (also referred to as ingrowth), growth and mortality of trees (Beers, 1962). Of these processes, growth is best understood and has been studied across a large variety of species and ecosystems (e.g. Hasenauer, 2006; Pretzsch, 2009; Burkhart and Tome, 2012, Rohner et al., 2018). Mortality has received increased attention in recent years (e.g. Hülsmann et al., 2017; Bugmann et al., 2019), after apprehensive increases of natural tree mortality were observed in many forest ecosystems around the globe (Allen et al., 2010; Neumann et al., 2017). As a result, increased tree mortality has led to increased efforts to more accurately represent tree mortality and tree recruitment in forest growth models (e.g. Ledermann, 2002; Zell et al., 2019), as both are crucial factors for long-term projections of forest dynamics under changing environmental conditions (König et al., 2022).

Sample-based models of forest dynamics are often initialised with tree diameter distributions originating from forest inventories. Hereby, tree recruitment is defined as trees that pass the inventory-specific size threshold (system property of the sampled tree population) over a defined period of time (model property, Tomppo, 2010). Historically, tree recruitment was simulated by applying a constant amount of recruitment trees (Weiskittel et al., 2011), assuming, e.g. sufficient homogenous natural regeneration after strip-cutting or planting preceding clearcuts. Such static approaches were sufficiently accurate when applied to e.g. stand table projections or matrix models in equilibrium (Vanclay, 1994). However, socioeconomic, political and environmental changes have promoted forest management shifts towards uneven aged, multi-species forestry systems in large parts of Europe (FOREST EUROPE, 2020). In those systems, rotation cycles do not exist anymore and heterogenous natural regeneration has become a more common source of forest regeneration (Mason et al., 2022). As a result, transient rather than equilibrium dynamics have become the rule, reflecting a broader ecological understanding that emphasizes the importance of transient states in ecosystem development (McCann, 2000).

Static recruitment models have therefore become less appropriate and necessitate the development of dynamic approaches that take into account variability in stand characteristics, forest management and changing site conditions, usually using regression techniques (Vanclay, 1994). These dynamic models have proven to be more accurate but, like the static models, would always predict recruitment numbers greater than zero which does not align with forest survey observations (Shifley et al., 1993). Furthermore, these models were not able to account for the large variation that is often observed in tree recruitment data. Tree recruitment remains a rare event, seemingly random, and does often not occur in a given period of time. Standard regression models, however, assume a rather small overdispersion. To tackle this issue, advancements have been made that simulate tree recruitment in two stochastic steps where, first, the probability of observing recruitment is modelled, and second, the amount of recruitment (cf. Adame et al., 2010; Ledermann, 2002). This approach was later refined into zero-inflated models, which combine the two probability functions of the two-step approach—one for modelling excess zeros and another for the count process—into a single framework. This allows for higher model fit and greater parameter parsimony by simultaneously estimating the probability of structural zeros and the count outcomes, providing a more accurate representation of datasets with many zeros (Fortin and DeBlois, 2007).

Dynamic tree recruitment models have been developed for a selection of single species (cf. Bravo, et al., 2008; Eerikäinen et al., 2014; Klopcic et al., 2012; Li et al., 2011; Moon et al., 2019; Mugasha et al., 2017; Yang and Huang, 2015; Zhang et al., 2012) and a few national modelling frameworks that include *multiple species* (cf. Ledermann, 2002; Zell et al., 2019; Flury et al., 2024). These national frameworks have in common that they are applied to forest ecosystems which are specific to *one* forest inventory sampling procedure. Applying such a model to a system with a different sampling procedure may not be feasible if the predicted recruitment trees' size threshold is smaller than that of the sampled trees, or it may introduce biases that compromise model predictions if the threshold is larger. A dynamic tree recruitment model, sensitive to the sampling procedure and size threshold of recruitment trees, has once been developed on a stand level using multiple regression techniques (Shifley et al., 1993). A large-scale dynamic tree recruitment model, sensitive to sampling procedures, does not exist. Combining data sets would broaden the environmental gradient, which is essential for enhancing the quantification of climatic influences on tree recruitment, as these influences have previously been only weakly detectable (cf. Zell et al., 2019; Käber et al., 2021; Flury et al., 2024).

In this study, data from over 95,000 permanent sample plots collected across eight European countries were utilized, encompassing various sampling procedures, environmental conditions, and nearly 138,000 individual tree recruitment events. A survey-sensitive, dynamic recruitment model was parameterized to simulate the count and species of recruiting trees in a two-step modelling approach, with a specific focus on previously weakly detectable or undetectable climatic effects (Käber et al., 2021; Zell et al., 2019). The influence of forest management, forest structure, soil characteristics, nutrient deposition, and five groups of weather and climate variables, including annual averages, intra-annual averages, annual variability, intra-annual extremes, and combinations thereof, were tested on both the quantity and species composition of recruiting trees. To emphasize climatic and forest structural effects, species-specific responses were omitted from the recruitment count model, as their impact diminishes with increasing size thresholds, unlike in regeneration, and were instead accounted for in the species model.

The study aimed to accomplish the following objectives: (I) evaluate the predictive accuracy of recruitment in relation to different sampling procedures and (II) quantify environmental and management factors that influence recruitment. By achieving these goals, the research contributes to the development of robust and dynamic simulations of tree recruitment in European forest surveys. It is tailored towards the implementation into the European Forest Information Scenario Model EFISCEN-Space (Lerink et al., 2023; Schelhaas et al., 2018) and presents a reproducible method that can also be applied to other empirical forest growth modelling frameworks. This would decrease their specificity to the sampling method and, hence, increase their applicability and sensitivity to climate impacts.

2. Materials and methods

2.1. Data

All the data for this study was obtained from repeated forest inventories, mostly National Forest Inventories (NFI, Table 1). For the Czech Republic, we used the CzechTerra Landscape Inventory (Cienciala

Table 1

Forest inventory overview per country. Plot overlap refers to the number of repeatedly measured plots between two subsequent censuses. Tree and recruitment observations refer to overlapping plots.

Country	Census period	Plot overlap	No. of trees	No. of recruits
Belgium, Flanders	1997–1999		14,816	
	2009–2018	689	17,337	4009
Belgium, Wallonia	1994–2004		13,155	
	2008–2011	1221	16,927	535
Czech Republic	2008–2009		10,066	
	2014–2015	344	10,234	86
Finland	1985–1986		48,732	
	1995	2490	64,596	4719
The Netherlands	2001–2005		24,417	
	2012–2013	1307	35,496	7327
Poland	2005–2009		518,328	
	2010–2014	24,365	592,140	62,991
Spain	1986–1996		642,208	
	1997–2007	46,415	873,015	43,872
Sweden	2003–2008		270,759	
	2008–2013	13,762	309,963	8570
Switzerland	1993–1996		58,955	
	2004–2006	4442	63,522	5875
Total		95,035	3584,666	137,984

et al., 2016). From Finland a repeated forest inventory dataset (1985–86 and 1995) from the forest health monitoring network was used, for details see Mäkipää & Heikkinen (2003). The inventory design in Poland and The Netherlands allows plot sizes to vary between censuses, depending on the forest age or the number of trees. The tree observations of those plots were reduced to the minimum observed plot radius across the censuses and checked for spatial biases by visual inspection and consultation of the corresponding country experts. All data was put into a standard format for further processing (Esquivel-Muelbert, in prep.). One hundred and eighty-two tree species were recorded in the data set (Supplement 2). Because most species were observed rarely, we grouped them into species groups following the approach described by Schelhaas et al. (2018). A group was formed if a species was present in more than 5 % of the plot observations or formed an important commercial or regional species. Additionally, three rest groups were made for short-lived broadleaves, long-lived broadleaves and other conifers, resulting in 19 groups in total (Fig. 1, Supplement 2). Grouping the tree species allows sufficient amounts of observations in each group for adequate parameter estimation.

The dataset spans a total of 95,035 repeated plot observations with

the records of 3.5 M trees of which 137,984 were identified as recruitment trees (Table 1). For some countries more than two observations per plot were available. In this case we selected the observations that had the largest overlap in time with the remaining dataset. All forest inventories in our dataset consist of two or more concentric plots with different radii, except Poland and The Netherlands with a single circular plot. The size threshold for trees to be included in the sample varies between 4 and 12 cm diameter at breast height (DBH) among the inventory datasets. In the case of several concentric plots, recruitment refers to the trees which pass the DBH threshold of the smallest plot. Trees passing the DBH threshold of the larger plots are referred to as ongrowth and are not part of this study (Beers, 1962). Country-specific differences between the size of the smallest plot, the DBH threshold and the average time interval between two observations are recorded in Table 2.

The dependent variables, quantity of recruitment trees per plot ($n.in$) and the species of recruitment trees ($in.sp$) were, together with the forest structural variables, directly derived from the inventory data. Forest structure was represented by six variables calculated at the first census at plot level: basal area of living trees per hectare ($ba.alive$), basal area of trees removed from the sampled tree population between the censuses per hectare ($ba.dead$, cause of death unknown), number of living trees per hectare ($n.ha$), distribution of observed basal area per hectare ($ba.skew$), lead species in a plot based on the basal area share of living trees ($lead\_sp$), and forest type, a categorical variable with two levels ($forest.type$, single-species stand or multi-species stand depending on the number of species observed at plot level). For the calculation of unbiased numerical forest structural variables only trees with a DBH $\geq$ 12 cm were used (equal to the largest DBH threshold in the dataset, see Table 2). Basal area (BA) at tree level was calculated from the DBH measurements using the standard formula: $basal\ area = \pi\left(\frac{DBH}{2}\right)^2$, where DBH is the diameter at breast height. The total basal area per plot was obtained by summing the individual tree basal areas within the plot (for living and dead trees separately). Basal area skewness was calculated at plot level after Pearson's coefficient of skewness using the formula: $basal\ area\ skewness = \frac{3(Mean - Median)}{Standard\ deviation}$.

Soil characteristics were derived from the SoilGrids dataset which consists of nine variables at seven different soil depths with a resolution of 1 km (Hengl et al., 2014). From the available variables we included only cation exchange capacity (Forzieri et al., 2021) and the percentage of silt content at a soil depth of 15 cm ($SLTTPT$) because of high collinearity between the variables and between the soil depths. Nutrient deposition was represented by reduced nitrogen ($RedN$) from the EMEP
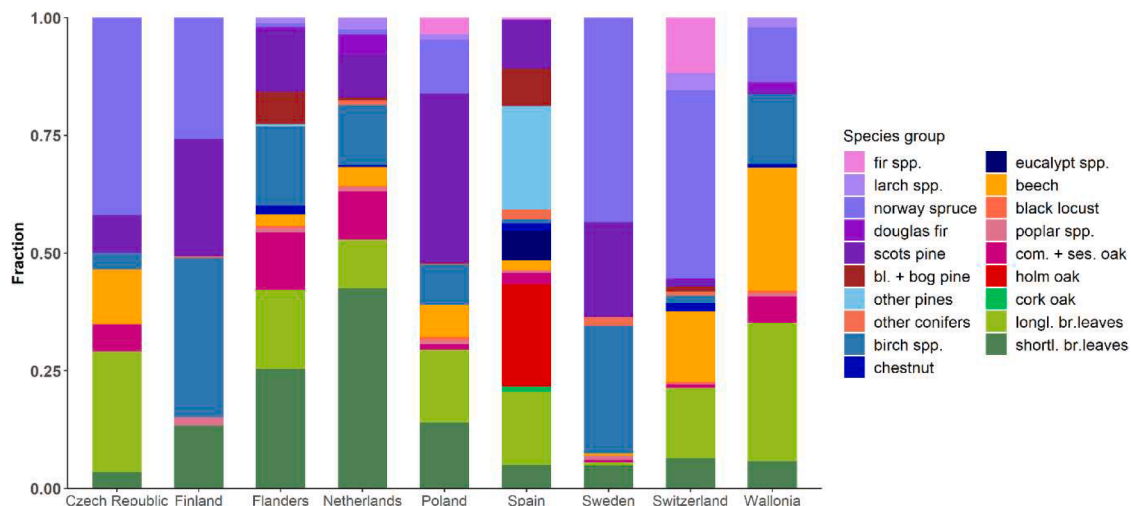

Fig. 1. Species group composition of tree recruits across countries. A table with percentages per species group and country is presented in Supplement 4.

Table 2

Sampling procedures and country-specific recruitment characteristics: DBH threshold, mean plot area and mean time interval between observations of the smallest circular plot and corresponding mean observed plot tree recruitment and the percentage of plots without tree recruitment. Numbers in brackets show the standard deviations.

Country	DBH threshold [mm]	Mean plot area [m2]	Mean time interval [years]	Mean plot recruitment [trees/plot]	Plots without recruitment [%]
Belgium (Flanders)	70	254 (0)	14.5 (2.6)	5.82	15.5
Belgium (Wallonia)	64	64 (0)	10.7 (3.6)	0.44	79.8
Czech Republic	70	28 (0)	5.9 (0.3)	0.25	85.5
Finland	46	100 (0)	9.8 (0.4)	1.9	45.3
Netherlands	50	329 (245)	9.6 (1.6)	5.61	28.3
Poland	70	274 (96)	5 (2)	2.59	50.6
Spain	75	79 (0)	11.2 (0.9)	0.95	63
Sweden	40	38 (0)	5 (0.2)	0.63	72.8
Switzerland	120	197 (18)	10.9 (1.1)	1.33	54.9

data set at a grid of 50 km^2 (EMEP, 2021) for which we calculated the average from 1990 to 2010 (Table 2).

Daily weather data was obtained from the Agri4Cast system (JRC, 2021) with a resolution of 25 km for the period 1985 to 2019. We extracted monthly values of mean temperature, total precipitation, total potential evapotranspiration and total radiation to calculate the mean, minimum, maximum and standard deviation at different temporal aggregation levels (monthly, warmest quarter, coldest quarter, driest quarter, wettest quarter and annual) and additionally six weather indices (Supplement 1). All variables were calculated for the specific period between two observations at the plot level. A detailed description is provided in (Schelhaas et al., 2018). The weather variables were complemented with climatic variables obtained from WorldClim (Hijmans et al., 2005), GEnS (Metzger et al., 2013), based on

Table 3

Description of response and explanatory variables. In subsequent analyses the base variables were combined separately with the variables from group 1–5. Group 5 forms a combination of uncorrelated variables from group 1–4. The mean and standard deviation are shown before transformation and standardisation. The variables listed under NFI method were only used to model the quantity of recruitment trees and not the species of recruitment trees.

	Category	Variable	Abbreviation	Unit	Mean (± std)
Base variables	Response	Number of recruitment trees per plot between two observations	n.in	n	1.45 (±3.72)
		Species group of recruitment trees	in.sp	class	
	Inventory method	Time in decimal years since last observation (modelled as offset)	interval	years	8.62 (±3.29)
		Plot area of the smallest circular plot (modelled as offset)	plot.area	m2	133.55 (±109.69)
		DBH threshold (dbh) transformed to dbh' = ln(dbh)	dbh'	mm	69.45 (±16.74)
	Forest structure	Stem number of living trees per hectare (n.ha) transformed to n.ha' = log(n.ha+1)	n.ha'	n/ha	403.58 (±330.57)
		Basal area of living trees per hectare (ba.alive) transformed to ba.alive' = sqrt(ba.alive)	ba.alive'	mm^2/ha	18.3 (±14.27)
		Basal area of removed trees per hectare (ba.dead) transformed to ba.dead' = ln(ba.dead+1)	ba.dead'	mm2/ha	2.51 (±5.73)
		Basal area distribution of living trees calculated as Pearson's coefficient of skewness	ba.skew	index	0.77 (±0.84)
		Forest type with two levels (single species stand, multi-species stand)	forest.type	class	n.mixed = 55,522, n.mono = 39,515
		Lead species group in a plot based on basal area ($n = 19$)	lead_sp	class	
	Soil	Cation exchange capacity	CEC	cmol kg^{-1}	16.04 (±3.84)
		Silt content mass fraction	SLTPPT	%	29.7 (±5.32)
	Deposition	Deposition of reduced nitrogen	RedN	mg(N) m^{-2}	516 (±342)
Group 1 Annual averages	Weather	Annual average of monthly mean temperatures	w_MaT	C	10.39 (±4.05)
		Total annual precipitation	w_TaP	mm	555 (±198)
		Thornthwaite 1948 humidity index	w_ThHUi	index	126.94 (±57.18)
	Climate	Annual actual evapotranspiration	c_TaAET	mm	505.24 (±99.99)
Group 2 Intra annual averages	Weather	Mean monthly temperature of wettest quarter	w_MweqT	C	12.49 (±3.09)
		Mean monthly temperature of warmest quarter	w_MwaqT	C	19.12 (±3.29)
		Mean monthly precipitation of driest quarter	w_MdrqP	mm	19.71 (±11.63)
	Climate	Total precipitation for months with mean monthly temperature above freezing point	c_Tmm0P	mm	606 (±216)
Group 3 Annual variability	Weather	Average annual diurnal temperature range	w_MaDR	C	9.5 (±2)
		Standard deviation of monthly mean temperature	w_SDmT	C	6.98 (±1.25)
		Standard deviation of monthly precipitation	w_SDmP	mm	32.63 (±10.08)
		Standard deviation of monthly radiation	w_SDmR	GJ m^{-2}	217.96 (±13.96)
	Climate	Seasonality of precipitation	c_seaP	mm	31.53 (±11.08)
		Seasonality of potential evapotranspiration	c_seaPET	index	4624 (±637)
Group 4 Intra annual extremes	Weather	Mean temperature of warmest month	w_MAXmT	C	20.47 (±3.2)
		Precipitation of wettest month	w_MAXmP	mm	116.49 (±36.46)
		Precipitation of driest month	w_MINmP	mm	9.14 (±7.19)
	Climate	Minimum precipitation in Dec. Jan. Feb.	c_MINdjbP	mm	46.05 (±25.2)
Group 5 Combined selection	Group 1	Thornthwaite 1948 humidity index, Annual actual evapotranspiration,			
	Group 2	Mean monthly temperature of wettest quarter, Total precipitation for months with mean monthly temperature above freezing point			
	Group 3	Average annual diurnal temperature range, Standard deviation of monthly mean temperature, Standard deviation of mean radiation, Seasonality of precipitation, Seasonality of potential evapotranspiration			
	Group 4	Mean temperature of warmest month, Precipitation of wettest month, Precipitation of driest month			

WorldClim) and CGIAR-CSI (Trabucco et al., 2008; Zorner et al., 2008) averaged over the period 1950 - 2000 at a resolution of 1 km (Table 3). A total of 103 biotic and abiotic covariates consisting of forest structural variables and gridded soil, nutrient deposition, weather and climate variables were compiled to explain patterns in the quantity and the species of recruitment trees (full list of considered variables in Supplement 1).

2.2. Statistical analyses

A data-driven model selection approach based on Maximum Likelihood estimates was chosen. This so-called Information-Theoretic Model Selection (I-T) encourages the examination of multiple alternative models, contrasting the classical null hypothesis significance testing (Newland, 2019). This approach enabled the testing of a comprehensive set of collinear explanatory variables in separate models, facilitating the exploration of alternative hypotheses. For instance, the investigation focused on determining whether tree recruitment is primarily driven by averaged climate variables, climatic variability or if it is influenced to a greater extent by climatic extremes (maximum and minimum values).

First, base variables were selected that contained only the forest structural, nitrogen deposition and soil variables (Table 3). An interaction effect was included between the basal area of living trees and stem density to account for different development stages of the forest. From the full set of available variables (Supplement 1) a stepwise removal of variables with a variance inflation factor (VIF, Zuur et al., 2010) larger than 4 was performed, removing the variable with the largest VIF, first. The Pearson and Spearman correlation coefficients was additionally checked between variables to detect potentially remaining collinearity issues.

Collinearity was highest between the weather and climate variables because most variables differ only in their spatial and temporal resolution. For example, the mean annual temperature of the weather dataset was strongly correlated with the mean annual temperature of the climate dataset (Pearson correlation coefficient $r= 0.96$). In case a variable was present in both datasets, we included the weather variable due to the higher temporal resolution and the expected direct effect on tree development. But collinearity was also present within the weather and the climate datasets. A typical example in the weather dataset is the mean annual temperature which correlates strongly with the mean temperature of the warmest quarter of the year ($r= 0.95$), the standard deviation of monthly mean temperature ($r = -0.72$) and the temperature of the warmest month ($r= 0.94$). Therefore, we grouped the weather and climate variables into four groups: annual averages, intra annual averages, annual variability and intra annual extremes (Supplement 1). The number of variables in those groups was, in combination with the base variables, further reduced based on VIF. A fifth group was formed based on the combined selection of the previous four groups. Final selection of retained variables in this group was, similar to the previous groups, based on a stepwise selection based on the VIFs (Table 3).

2.2.1. Modelling the quantity of recruitment trees

Tree recruitment is a rare event, hence, recruitment data is often zero-inflated (Table 2, Supplement 3). Discrete probability (count) distributions like the Poisson and Negative Binomial distributions can generally model data with large zero counts. The Negative Binomial is more flexible because its probability mass function contains two parameters in contrast to the Poisson probability mass function with one parameter. We combined the base variables separately with the five weather and climate groups (Table 3) and fitted a Poisson and a Negative Binomial model, resulting in 10 different combinations. In case of presence of overdispersion (e.g. high number of zeros) we expanded the Poisson to the zero-inflated Poisson model (Zuur & Ieno, 2012). We additionally fitted models to the base variables to compare those fits to models, including climate and weather variables. Thereafter, we performed a backward selection of the full models based on the Akaike

Information Criteria (AIC; Burnham and Anderson, 2002) to remove uninformative covariates. We fitted the models with the "glmmTMB" package (Brooks et al., 2017) in R (Core Team, 2022).

The probability of observing recruitment in a plot increases with plot size and time between the measurements but decreases with a higher DBH threshold (cf. Table 3, Fig. 2). The DBH threshold was included as a covariate to account for differences between NFIs, while plot area and time interval between observations were included as offsets. An offset assumes a coefficient of 1 to ensure a proportional effect or to maintain a rate. Efforts to account for country-specific sampling methods by incorporating a random effect at the country level or by defining plot area and interval as fixed factors with an interaction effect between them, as recommended by Feng (2022), failed to reduce residual patterns or enhance model fit. All forest structural variables were normalised using transformations (cf. Table 3). Due to the non-linear relationship between standardized plot recruitment and increasing diameter thresholds (cf. Fig. 2), we compared a logarithmic model (log (x)) and a square root model (sqrt(x)), using least-squares regression. The logarithmic model provided a better fit, with a lower RMSE (1.1707) compared to the square root model (RMSE: 1.2337). Based on these results, we describe the relationship as a logarithmic decline and have included the log-transformed diameter threshold in the analysis. To prevent computational problems while fitting the models, all covariates were scaled to a mean of 0 and a standard deviation of 1. The regression equation is represented as

$$\log(y) = \beta_0 + \beta_1 x_1 + \beta_2 x_2 + \ldots + \beta_k x_k +$$

$$\log(plot.area) + \log(interval) + \varepsilon,$$

where y represents the recruitment abundance, modelling the mean of a Poisson distribution or a Negative Binomial distribution with a log-link function. $x_1, \ldots x_k$ denote the k covariates and ε the independent and identically distributed error term. Furthermore, in the context of zero-inflated models, the probability of a zero, denoted with π, is modelled with

$$\log\left(\frac{\pi}{1-\pi}\right) = \beta_0 + \beta_1 x_1 + \beta_2 x_2 + \ldots + \beta_k x_k +$$

$$\log(plot.area) + \log(interval) + \varepsilon.$$

The significance of model parameters was assessed using the Wald test, which evaluates the contribution of each predictor to the model fit based on its estimated coefficient and standard error (Bolker et al., 2009). To evaluate the model, we generated 1000 random datasets from the fitted model's distribution and compared their distributions to the observed data, assessing the model's ability to accurately capture recruitment dynamics. The model was validated using bootstrapped cross-validation with 100 resamples based on deviance residuals calculated with the R-Package "DHARMa" (Hartig, 2024). This approach allows to assess the model's robustness, providing a measure of its performance on unseen data (Zuur and Ieno, 2012).

2.2.2. Modelling the species composition of recruitment trees

We fitted a multinomial logistic regression model (MLRM) to model the probabilities of each of the 19 recruitment species groups (cf. Zell et al. 2019). MLRMs optimize the regression equation for each group simultaneously. The probability p_i of observing species group i with reference category J is given as:

$$p_i = \frac{\exp(\beta_{i,0} + \beta_{i,1} x_1 + \beta_{i,2} x_2 + \ldots + \beta_{i,1} x_k)}{1 + \sum_{j=1}^{J-1} \exp\left(\beta_{i,0} + \beta_{j,1} x_1 + \beta_{j,2} x_2 + \ldots + \beta_{j,1} x_k\right)}$$

And the probability to be in the reference category is given as:

$$p_J = \frac{1}{1 + \sum_{j=1}^{J-1} \exp\left(\beta_{i,0} + \beta_{j,1} x_1 + \beta_{j,2} x_2 + \ldots + \beta_{j,1} x_k\right)}$$
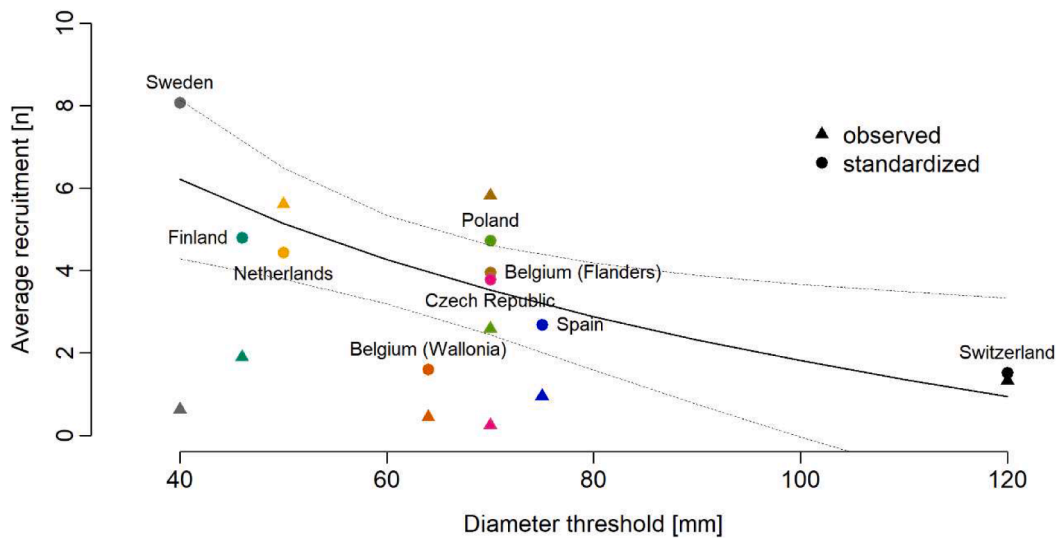
Fig. 2. Average observed (triangles) and standardised (dots) plot recruitment per country over country-specific diameter thresholds. Plot recruitment was standardized by adjusting for differences in plot size and time interval. Recruitment values were scaled to a reference plot size of 500 m² and a 5-year time period. After standardizing all plots, the recruitment data were averaged across the entire country. The relationship between the standardised average plot recruitment and the DBH threshold can be approximated with a negative log function (logistic regression line and 95 % confidence intervals: black lines).

where β_i the species group specific regression coefficients, and $x_1, \ldots, x_k$ the covariates. We calculated the probability of each species group relative with these equations. The exponentiated linear combination of the regression coefficients and covariates in the numerator represents the odds of the specific outcome occurring, and the denominator ensures the probabilities sum up to 1 across all outcome categories.

Even though model assumptions regarding collinearity are more relaxed in MLRs, we fitted a separate model for each of the five weather and climate groups (cf. Table 3). In contrast to the discrete probability distributions used for the quantity of tree recruits, variables linked to the sampling design were removed due to perfect separation between the species groups which would lead to a violation of MLRM model assumptions. Uninformative covariates were removed based on the AIC (Burnham and Anderson, 2002). The models were fitted using the function "multinom" from the "nnet" package (Venables and Ripley, 2002). The final model was validated using 10-fold cross-validation to assess its predictive robustness (Arlot and Celisse, 2010).

To gain insights into the effects of the numerical covariates across the entire dataset, we estimated the average marginal effects (AMEs) in the species model. This was achieved using numerical perturbation by adding a small value ($\delta = 1 \times 10^{-5}$) to each covariate. Predicted probabilities were computed for both the original and perturbed data, and the change in probabilities was divided by δ to approximate the marginal effect. The results were then averaged across all observations, representing the change in predicted probability per one standardized unit change in the covariate. The categorical variables, forest type and lead species group, were retained as observed in the data (cf. Fig. 5).

3. Results

3.1. Recruitment count model

The Poisson models were unable to account for the observed zero-inflation of recruitment counts in the dataset (Table 4). The zero-inflated Poisson models reproduced the number of zeros best but were outperformed by the Negative Binomial models in all 5 model categories. Because the Negative Binomial models were able to handle the dispersion of the data, those models were not extended to zero-inflated models. In general, differences between the performances of the 5 model groups was small (Table 4). Based on the AIC, the best performing model

Table 4

Performance overview of the recruitment count models: the number of factors retained in the model (for the zero-inflated models the number of variables are split up into the conditional model and the zero-inflation model in brackets); the Akaike Information Criteria (based on the maximum likelihood); the AIC differences to the lowest AIC; and the ratio between the average number of zeros in 1000 simulated datasets and the observed number of zeros (56,893).

	Distribution	Factors	AIC	deltaAIC	Zeros
Base model Forest structure	Poisson	9	407,439	143,825	0.66
	Zero inflated Poisson	9 (8)	337,648	74,034	1.00
	Negative Binomial	9	266,636	3022	1.01
Model 1 Annual averages	Poisson	15	397,239	133,625	0.67
	Zero inflated Poisson	14 (12)	331,822	68,163	1.00
	Negative Binomial	13	264,686	1072	1.01
Model 2 Intra annual averages	Poisson	15	391,907	128,293	0.69
	Zero inflated Poisson	13 (12)	327,513	63,899	1.00
	Negative Binomial	14	264,054	440	1.01
Model 3 Annual variability	Poisson	16	395,035	131,421	0.68
	Zero inflated Poisson	16 (14)	329,111	65,497	1.00
	Negative Binomial	15	264,504	890	1.01
Model 4 Intra annual extremes	Poisson	15	396,786	133,172	0.68
	Zero inflated Poisson	15 (11)	330,480	66,866	1.00
	Negative Binomial	14	264,653	1039	1.01
Model 5 Combined selection	Poisson	18	390,049	126,435	0.69
	Zero inflated Poisson	19 (16)	325,985	62,371	1.00
	Negative Binomial	17	263,614	0	1.01

was group 5 with a Negative Binomial distribution (Table 4). The model did not fit to all countries equally well (cf. Supplement 3). Further results are shown for group 5, the results of group 1–4 are recorded in Supplement 5. The semivariance of the model was low, indicating no issues with spatial autocorrelation of the residuals (see semivariogram in Supplement 6). The results of the bootstrapped cross-validation showed

an average deviance residual of 0.496, indicating that the model predictions align well with the observed data. The bias (-0.00027) was nearly negligible, suggesting that the model does not systematically overestimate or underestimate predictions. Additionally, the standard error (0.00063) was very low, reflecting high consistency across the bootstrap resamples and confirming that the model provides stable and reliable estimates. These results support the robustness of the model and its ability to generalize to new data.

Except for the lead species group and skewness of basal area, all forest structural variables (*forest.type, n.ha', ba.alive', ba.dead'*) as well as soil and depositions variables (*CEC, SLTPPT, RedN*) were informative (Table 5). From eleven climate and weather variables, seven were retained. Those variables originated from all four weather and climate categories (cf. Table 3). Total annual actual evapotranspiration (*c_TaAET*), total precipitation for months with a mean temperature above freezing point (*c_Tmm0P*), the standard deviation of monthly mean temperature (*w_SDmT*), and monthly mean radiation (*w_SDmR*) did not improve model performance and were removed from the final model.

The small differences between the performances of the five models (Table 4) in combination with the effect size of the parameters (Table 5) shows that the number of recruitment trees is largely determined by forest structure. The strongest effect was found for the basal area of living trees and the stem density. Both function as a proxy for stand density, controlling the amount of resources available for the regeneration, such as light, water and nutrients.

The largest effects of weather and climate variables were found for variability and extremes of temperature and precipitation (cf. Table 5, Fig. 3K–P). The results illustrate the sensitivity of tree recruitment to

Table 5
Coefficients of the tree recruitment count model 5 (combined variables, using a Negative Binomial distribution). Confidence intervals and p-values were computed using a Wald-test.

Category	Variable	Coefficient	95 % CI	Pr (>|z|)
Forest structure	forest.type (multi-species stand, Intercept)	-6.703	[-6.722, -6.684]	< 0.001
	ba.alive' (square root transformed)	-1.202	[-1.224, -1.180]	< 0.001
	ba_dead' (log transformed)	-0.322	[-0.335, -0.309]	< 0.001
	forest.type (single-species stand)	-0.779	[-0.807, -0.751]	< 0.001
	n.ha' (log transformed)	1.182	[1.151, 1.213]	< 0.001
	ba.alive' X n.ha'	0.344	[0.330, 0.358]	< 0.001
Inventory method	DBH threshold (log transformed)	-0.123	[-0.144, -0.102]	< 0.001
Soil and deposition	Deposition of reduced nitrogen	0.052	[0.035, 0.069]	< 0.001
	Cation exchange capacity	-0.116	[-0.134, -0.098]	< 0.001
	Silt content	0.063	[0.046, 0.08]	< 0.001
Weather and climate	Thornthwaite 1948 humidity index	-0.101	[-0.12, -0.082]	< 0.001
	Average annual diurnal temperature range	-0.093	[-0.116, -0.07]	< 0.001
	Mean monthly temperature of wettest quarter	0.224	[0.204, 0.243]	< 0.001
	Mean temperature of warmest month	-0.245	[-0.268, -0.222]	< 0.001
	Precipitation of wettest month	0.22	[0.201, 0.239]	< 0.001
	Seasonality of precipitation	-0.204	[-0.224, -0.184]	< 0.001
	Seasonality of potential evapotranspiration	0.052	[0.033, 0.07]	< 0.001

temperature and precipitation. While higher temperatures in the wettest quarter in the year facilitate recruitment, higher mean temperatures of the warmest month (observed during summer) limit recruitment. Further, higher numbers of tree recruits are expected with increasing precipitation of the wettest month. High precipitation seasonality, however, reduces the amount of expected recruitment.

3.2. Species model

Similar to the recruitment count model, the performance of the five multinomial logistic regression models differed strongly between Model 5 and the remaining models (Table 6). None of the models with distinct climate and weather groups outperformed another regarding accuracy. Model 5, which included a combination of variables from Model 1–4, performed best and was further investigated (Table 6). The average accuracy from the cross-validation was 65.18, while the full model trained on the entire dataset achieved a slightly higher accuracy of 65.37. The minimal difference between these values (0.19) indicates that the model generalizes well and is not overfitting to the training data. This consistency between the cross-validated performance and the full model performance highlights the model's predictive robustness. The full set of parameters is reported in Supplement 7. The most important set of variables to predict the species probabilities was forest structure, particularly the lead species of a plot, followed by weather and climate variables (Fig. 4, Supplement 7).

The largest contribution of a single variable to predict the recruitment species probabilities in a plot was the leading species group. The recruitment probability was highest for the leading species group in that plot (see also Supplement 7), showing that seed limitations play the most important role for species recruitment. This is also reflected in the effect of the categorical variable *forest.type*. The share of broad-leaved species and the diversity of recruiting species in general was higher in multi-species stands compared to single species stands, independent from weather and forest structural variables (Fig. 4A.1). An example of the model's sensitivity to climate is given in Fig. 4B1. The recruitment probability of *Picea abies*, for instance, declines from over 75 % at a mean temperature of the warmest month of 10 °C to below 20 % at 25 °C in spruce-dominated forests, a trend that was present across all shown leading species groups. Thermophilic tree species profited from higher temperatures such as *Robinia pseudoacacia* and *Abies* species. The share of broad-leaved tree species groups increased consistently with increasing temperatures across all leading species groups. Upon closer examination of the effect of forest structural variables, we observe clear differences in recruitment probabilities between shade-tolerant and pioneer species under varying stand densities. Shade-tolerant species such as *Abies alba* and moderately shade-tolerant species like *Picea abies* and *Fagus sylvatica* show higher recruitment probabilities with increasing basal area, while pioneer species like *Pinus sylvestris* and *Betula* species benefit from lower basal area values (cf. Fig. 4C.1 & Fig. 5).

4. Discussion

4.1. Climatic constraints of tree recruitment

Even though strong evidence of climatic effects on tree regeneration processes is present, few studies have investigated such effects in the context of tree recruitment (Price et al., 2001; König et al., 2022). Zell et al. (2019) and Käber et al. (2021) provide rare examples of tree recruitment modelling in combination with climate. Nevertheless, both studies found weak climatic effects. Käber et al. (2021) provide three possible explanations which we shortly introduce here to further the discussion on tree recruitment responses to climate and potential shifts under climate change: (1) geographic ranges of the study areas are usually small which may result in insufficient variation among climate variables and, hence, the lack of significant effects; (2) ontogenetic shifts
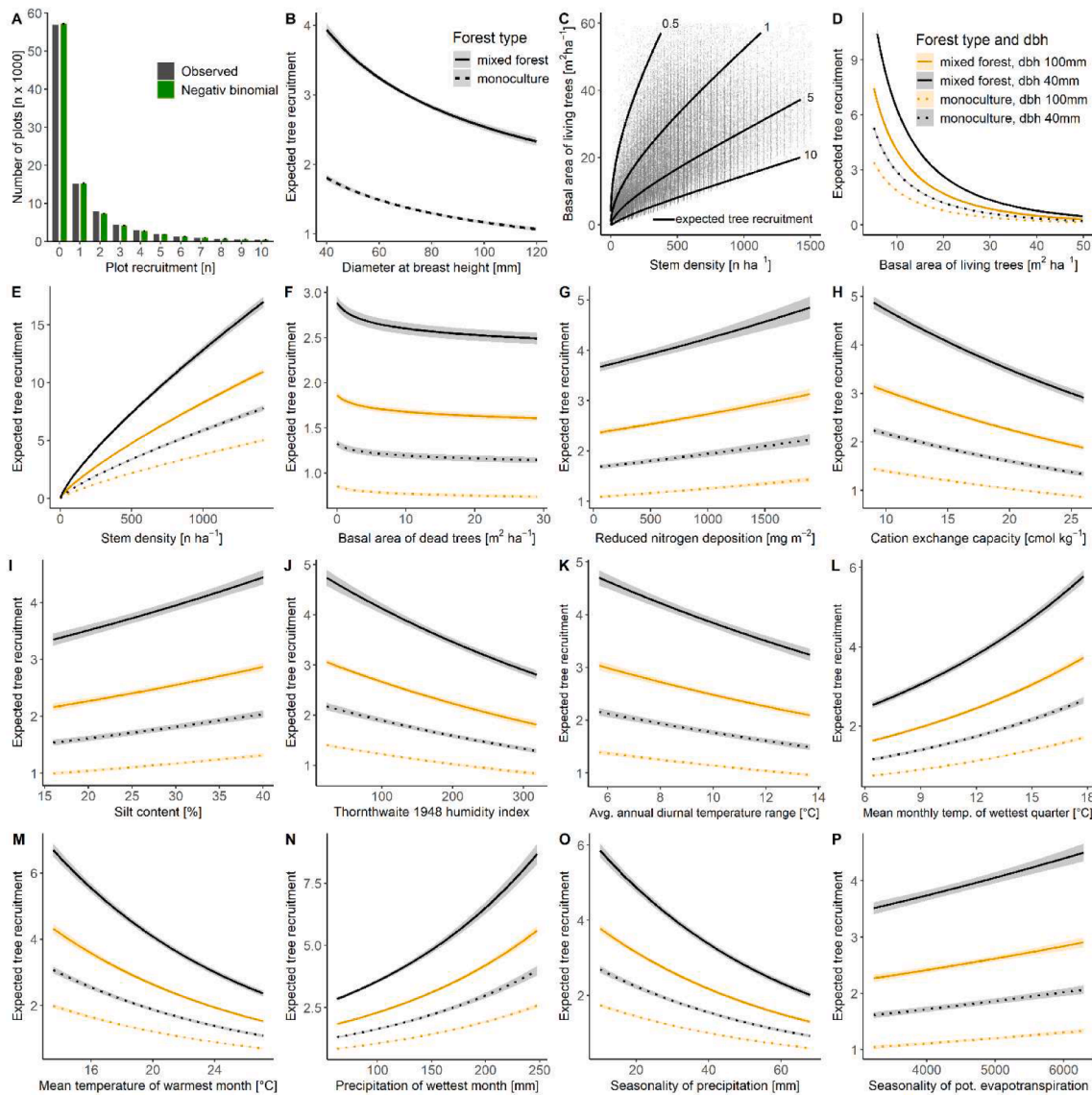
Fig. 3. Simulation results of the final Negative Binomial recruitment count model. A) Observed (black) and simulated plot recruitment (green = Negative Binomial) with standard errors. Plot recruitment was derived from the average of 1000 simulated datasets. B-P) Expected recruitment count (mean of the Negative Binomial distribution) on 500 m² and a 5-year period. B) Expected recruitment count over diameter threshold for mixed forests (solid line) and monocultures (dotted line). C) Visualisation of interaction effect between basal area and stem density on the expected recruitment counts. Dots show observed plot values. D-P) Expected recruitment count over the 1–99 % percentiles of retained variables. Predictions are shown for the two levels of forest type and two diameter thresholds (40 mm = black, 100 mm = yellow).

Table 6

Model performances of the different species models. The null model contains only an intercept. Given are the effective degrees of freedom (EDF) together with the Akaike Information Criterion (AIC) and the model accuracy. Model accuracy was assessed with 10-fold cross-validation.

	EDF	AIC	deltaAIC	Accuracy
Model 1 Annual averages	558	310646	6444	64.76
Model 2 Intra annual averages	558	311477	7275	64.60
Model 3 Annual variability	594	311952	7750	64.81
Model 4 Intra annual extremes	558	312831	8629	64.65
Model 5 Combination	684	304202	0	65.37

at young tree ages, meaning that trees may regenerate sensitive to climate but die off before they reach the required size threshold to be recorded as recruits; (3) micro-climate is more important than the climate outside the forest stand.

The strong and consistent climate effects, found in this study, supports the hypothesis of insufficient geographical coverage in past studies for the detection of significant climatic influence. The range of the 2.5th and 97.5th percentile of mean annual temperature in this study, for instance, is almost twice as large as the range covered by Zell et al. (2019). Combining forest data across countries is essential to broaden the range of environmental factors, which allows for a more robust quantification of their effects. Analysing each country separately would limit this capability due to the narrower environmental ranges within individual countries (see Supplement 8 for country-specific ranges of environmental covariates).

Our information-theoretic approach revealed that none of the distinct climate variable groups outperformed another and that the best model performance was achieved by the combined group. Collinearity between the groups in combination with the spatial resolution was assumed to be too high to detect large differences. Alternatively, all groups may contain equally influential variables that describe driving recruitment processes. The chosen combination of variables from
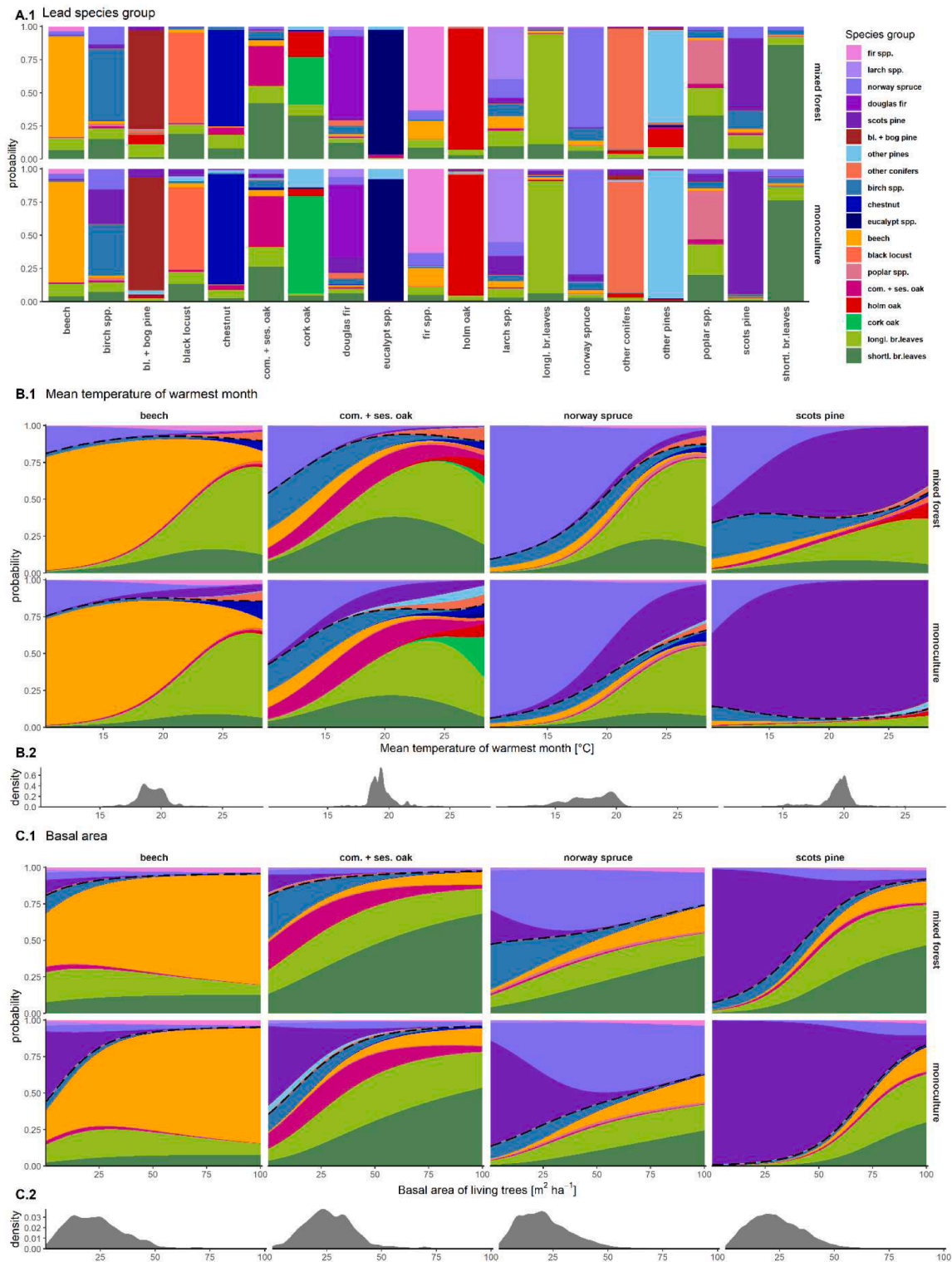
Fig. 4. Predicted species group probabilities for three variables of the species model 5 (A.1, B.1, C.1) for both forest types (mixed forest, monoculture). The effects of continuous variables on the predicted probabilities are shown for four levels of the categorical variable lead species (main timber species in Europe: beech, common and sessile oak, Norway spruce, Scots pine) while setting all other continuous variables to their mean. B.2 presents the distribution of maximum monthly temperature observations and C.2 for the observed basal area per hectare, respectively.

different groups preserves the potential to capture the latter explanation.

The results indicate that variables linked to drought and water limitations have a substantial effect on recruitment densities and species compositions. Higher recruitment densities are found in areas with high

and stable rainfall conditions. Further, while high temperatures in the wettest quarter of the year promote tree recruitment, high maximum temperatures form a limiting factor. Those patterns could be explained by processes linked to altered growth performances and mortality rates. Higher winter temperatures have been linked to higher growth rates of
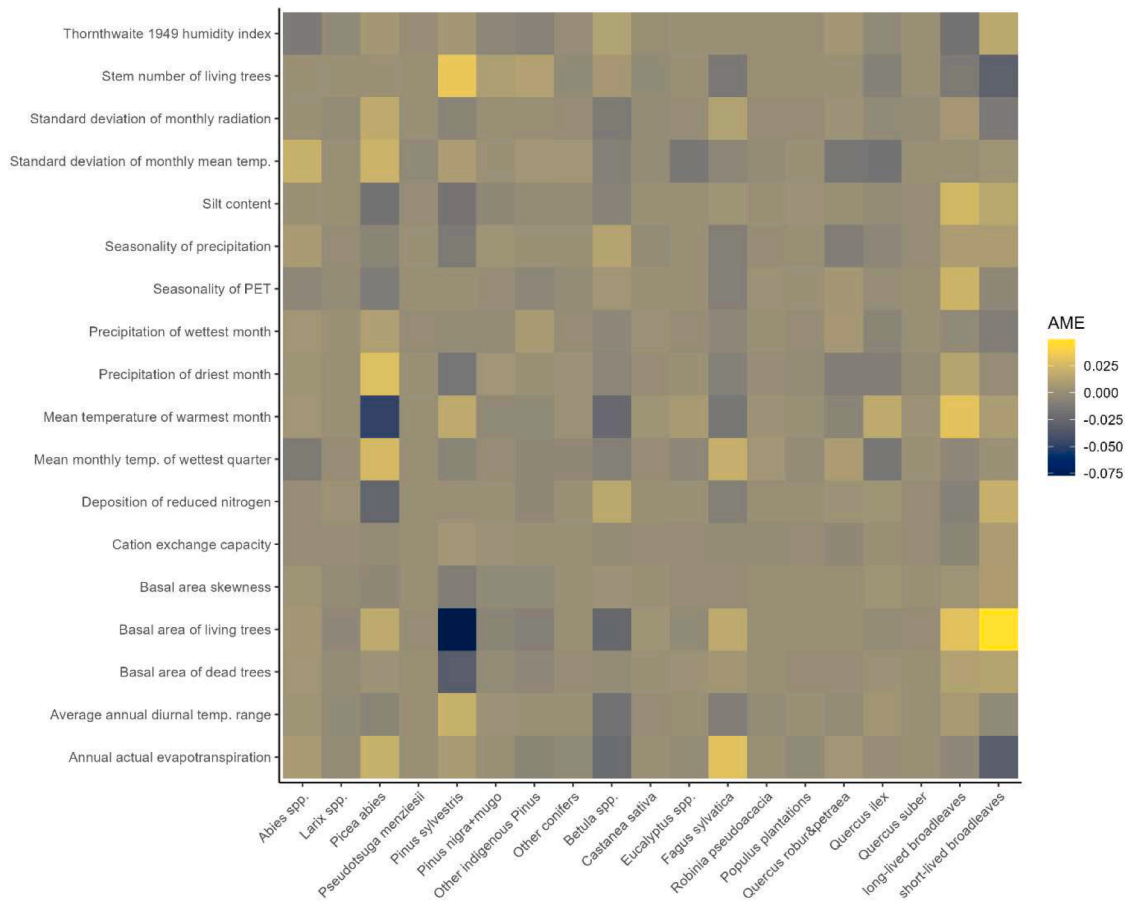
Fig. 5. Heatmap of Average Marginal Effects (AMEs) for different covariates across recruitment species. The AMEs represent the estimated change in predicted probability per one standardized unit change in each covariate. Positive values (yellow) indicate an increase in the probability of recruitment for a given species, while negative values (blue) indicate a decrease. Recruitment species are shown along the x-axis, and the covariates are listed on the y-axis.

adult trees (cf. Graumlich, 1991; Harvey et al., 2020; St George et al., 2010) which could have a positive effect on seed production (Koenig and Knops, 2000; Müller-Haubold et al., 2015). Simultaneously, young trees likely also benefit from better growth conditions due to increased resistance to natural disturbances while reaching the required size threshold in shorter time spans. The effects of maximum temperature and precipitation indicate that elevated mortality rates occur under dry conditions and strongly drive tree recruitment densities (Ibanez et al., 2007) but also shift the ratio between conifers and broadleaves. This is partly caused by the decline of *Picea abies* with increasing temperatures due to its vulnerability to drought due to its shallow root system (Lévesque et al., 2013). In contrast, many broadleaved species have deeper roots and more adaptive water management strategies, allowing them to survive and regenerate better under drier conditions (Kunz et al., 2018), thus giving them a competitive advantage in recruitment as temperatures rise and increasing their share among the recruits (cf. Figs. 4B.1 & 5).

4.2. Ecological or demographic process? The confounding effects of forest structure on tree recruitment

There is widespread agreement on the effects of forest structure on tree recruitment. The strongest influence is commonly found for the basal area of living trees (cf. Klopcic et al., 2012; Mugasha et al., 2017; Yang and Huang, 2015) which serves as a proxy for stand density and, hence, resource competition (Casper and Jackson, 1997; Feldmann et al., 2018). High values of basal area are usually associated with the presence of large trees and dense canopies. Such structures limit the availability of essential resources for successful tree regeneration like

the amount of light reaching the forest ground (Binkley et al., 2013; Kara and Topacoglu, 2018; Willson et al., 2020) and soil moisture (Dalsgaard, 2007; Marryanna et al., 2019; Metzger et al., 2017). However, the interpretation of forest structural variables demands caution. Not all forest structural variables follow ecological expectations but represent demographic processes. As pointed out by Käber et al. (2021) and Zell et al. (2019), the effect of basal area must be considered in combination with stem density. The combination of the two provides a good estimate for the development stage of a forest stand (Feldmann et al., 2018). While high basal area values and low stem numbers sketch the structure of mature and dense forest stands, low basal area and low stem number represents a young stand with high abundance of resources for tree regeneration.

Whereas forest ecologists would expect a negative effect of increasing stem density on the number of recruitment trees due to higher resource competition, the effect is positive (cf. Fig. 3C&E, Käber et al., 2021; Zell et al., 2019). Due to the lack of an ecological explanation, it is more obvious that the predicted increase of recruitment trees is linked to its demography. Recruitment trees have already successfully passed the vulnerable stages of tree seedlings and saplings (tree regeneration). Only years later, some of the regenerated trees may pass the size threshold to be recorded as recruitment, causing high stem densities at the plot level. However, more trees may yet just be below the threshold and pass the size threshold only in the subsequent observation which results in high recruitment under high stem densities. Stem density therefore forms a *demographic process* rather than an ecological one and does *not* represent the environmental conditions of the presence but shows that the environmental conditions in the past must have been favourable for the establishment of tree regeneration. This explanation is supported by the

fact that the stem density effect weakens with increasing basal area, hence, is only present in young forests (Fig. 3C). Even so, stem density forms a valuable variable in the context of recruitment modelling, not only because of its predictive power, but also because it ensures an ecologically correct interpretation of the basal area effect. Lastly, using stem density as driver of tree recruitment in a forest growth model requires the presence of a well-functioning mortality submodule that limits stem densities in relation to stand density (Pretzsch and Biber, 2005) to prevent the development of unrealistic forest structures in simulation studies.

A similar but less pronounced effect is found for the basal area of dead trees. While the ecological expectation of reduced stand density indicated by a high presence of dead trees would cause higher recruitment rates, the opposite was found. The most likely explanation is that the time delay between favourable conditions (lower basal area) and the presence of tree recruitment is too large to be captured between two consecutive plot observations. Recruitment trees regenerate years before they are measured. Hence, high basal areas of dead trees are more likely observed in dense stands with poor recruitment conditions and may cause a recruitment increase only later. Zell et al. (2019), who investigated the proportion of harvested basal area, directly accounted for the relationship between removed and living basal area and found only a weak positive effect. Within a few years, more than two consecutive plot observations will be available from National Forest Inventories which enables the investigation of effects of harvesting and mortality events further in the past. For now, an alternative explanation for the weak effect of basal area reduction could be linked to species-specific regeneration strategies. Shade-tolerant species tend to maintain seedling banks, meaning that a viable population of seedlings is available at all times. In case of unfavourable growing conditions, those seedlings die off and are replaced with a new population of seedlings in the subsequent year (Iida and Masaki, 2002; Shugart, 1984). If the growing conditions improve slightly, those seedlings grow into saplings which can persist for long time spans under unfavourable conditions. Low levels of basal area removal may already be sufficient to provide the resources needed for successful regeneration of shade-tolerant species. If stand density decreases fast, light-demanding pioneer species, dominantly relying on seed banks in the forest soil or cones, are outperforming shade-tolerant species and able to quickly colonise the new site (Tiebel et al., 2018). Given that tree regeneration may occur under both low and high levels of basal area reduction may explain the minor effect we found, as recruitment is possible under a wide range of stand density changes. While the regeneration density under light conditions is expected to be higher than that under shade, the recruitment density seems to equalise throughout stand development (Feldmann et al., 2018; Glatthorn et al., 2018; Pretzsch, 2009), so that no major recruitment density differences can be observed between the two situations. Käber et al. (2021) incorporated the level of light availability on the forest floor in their recruitment model and found distinct effects depending on the species' shade-tolerance which decreased with increasing tree size and coincides with our results that show species-specific recruitment success depending on the stand density (cf. Fig. 4C.1).

Lastly, the expectation of higher shares of broadleaved species in mixed forests compared to monocultures can be attributed to two main factors. First, niche differentiation allows diverse tree species to regenerate more effectively by reducing competition for resources such as light, water, and nutrients (Yan et al., 2015). This resource partitioning enables broadleaved and coniferous species to occupy distinct ecological roles, fostering denser and more successful regeneration (cf. Fig. 3). By optimizing resource use through these complementary niches, mixed stands support more vigorous recruitment than monocultures. Additionally, seed limitations contribute to this trend (Gilbert and Lechowicz, 2004). In mixed stands, where multiple *species* coexist, broadleaved trees, especially the long-lived species group, have a numerical advantage. This group alone includes over 30 species, many of

which hold economic value, suggesting that forest management practices may also play a role in promoting their regeneration (Supplement 2, Fig. 4).

4.3. Moderate influence of soil and nutrients on tree recruitment

The effects of soil variables on tree recruitment have rarely been studied in the context of tree recruitment modelling (cf. Käber et al., 2021; Zell et al., 2019). Base research on tree regeneration processes, however, revealed strong effects of soil moisture and nutrient availability on seedling regeneration and forest dynamics (Catovsky et al., 2002). Increased nitrogen availability, for instance, improves the growth performance of trees (Rohner et al., 2018) and leads to higher seed production rates. Nevertheless, the increased abundance of seeds is not necessarily converted into higher tree recruitment because of higher seed predation (Bogdziewicz et al., 2017) and seedling mortality, even though sapling growth shows positive effects (Catovsky and Bazzaz, 2002). The only weak positive effects of nitrogen deposition, cation exchange capacity and silt content found in this study are in line with the findings of Zell et al. (2019) and could be caused by a combination of missing species interactions (Proll et al., 2011) and the use of gridded soil and nutrient deposition data. Gridded data was required to achieve full coverage over the whole study area but might only roughly indicate the actual situation in a plot. Small-scale differences of soil factors might have a stronger influence on micro-habitats and, hence, the chance to observe tree recruitment.

The slightly positive effect of silt content, found in the present study, likely serves as an indicator of plant available water in the soil. The water holding capacity increases with silt content (Jabro et al., 2009) which may reduce drought stress of young trees and result in higher recruitment rates. Cation exchange capacity, however, revealed a counterintuitive effect. A negative effect on the density of tree recruits was found with increasing CEC. While CEC is a measure of nutrient availability for plant uptake and should subsequently promote tree performance and recruitment, a similar effect was found in a study on tree regeneration in Vietnam (Pham et al., 2022). The authors hypothesise that the positive relationship could be caused by a methodological artefact related to the soil depth at which CEC was measured which may not represent the real conditions of CEC. However, under the premise that a similar directional effect was found in our study, we propose an alternative explanation for the negative relationship. Increasing CEC may lead to increased competition with the herbaceous layer which also benefits from higher CEC (van der Waal et al., 2009) which in return causes positive feedback on ungulate densities and hence browsing pressure due to more nutritious foliage (Bowyer et al., 2014). A simulation study by Thrippleton et al. (2018) suggests that the effects of competition with the herbaceous layer in combination with browsing in European forests may lead to arrested forest succession. In summary, it is likely a combined effect, with nutrient-rich foliage enhancing browsing intensity, while competition with the herbaceous layer also significantly limits recruitment success. Overall, soil and nutrient related factors should receive more attention in further research with a focus on species-specific effects.

4.4. Constraints and ways forward for tree recruitment modelling across forest inventories

We acknowledge that the grouping of species in our model does not follow a biological rationale but rather reflects the commercial importance and frequency of the species groups, as this structure aligns with the forest resource model EFISCEN-Space. While this approach supports the model's current application, it mixes species with different regeneration biology, potentially affecting model performance, particularly for the rest groups "other conifers," "long-lived broadleaves," and "short-lived broadleaves." Future research should explore refined groupings based on taxonomical, ecological, or life history characteristics to better

capture species-specific recruitment dynamics and improve model accuracy.

The inconsistencies between survey methods regarding the time between the measurements, plot area and the measured tree sample (defined by the diameter threshold) evidently influences the amount of quantified tree recruitment (the actual amount of tree recruitment remains the same regardless of the threshold, but the amount of tree recruitment that is measured varies depending on the threshold used; cf. Tables 2 & 5). While the assumption of a proportional relationship between the measured plot area and the number of recruitment trees is reasonable, for time it likely only holds true under the premise that the values are not too widely distributed. More practically, given an observation of two recruitment trees on 250 m^2, it is acceptable to assume four recruitment trees on 500 m^2. Similarly, observing two recruitment trees in a five-year interval and assuming four recruitment trees in ten years is also acceptable. With increasing time between the measurements and subsequent proceeding stand development, however, it becomes more likely that some of the recruitment trees have been subject to harvesting or natural mortality. Further, with increasing time intervals, the relationship between tree recruitment and forest structural variables may weaken. Hence, if the time intervals become too extreme, the assumption of a proportional relationships between time or forest structural variable and the number of recruitment trees is increasingly compromised. The time intervals in this study were, with few exceptions, within ten years around the mean. Therefore, plot area and time interval were both modelled as offsets. However, adverse fits were found for Flanders and The Netherlands that resulted in undesired residual patterns (Supplement 3). While the expected effect of the diameter threshold was well captured (cf. Figs. 2, 3B), the remaining two factors of the sampling methods (plot area and time interval), set as offsets, were unable to capture the combined effect.

A more promising alternative to solve the described issues could be the application of non-discrete probability distributions after harmonising tree recruitment observations over time interval and plot area. The two major advantages are the prevention of collinearity issues between sampling variables and, with preceding interpolation, the ease of assumptions on plots where no recruitment was observed. While observed zeros stay always zeros, independent from the harmonisation method, interpolated recruitment rates stay within the limits of known plot areas and time intervals, in contrast to extrapolated rates. More practical, while it is unlikely that an observed zero on a 50 m^2 plot remains a zero if one hectare was observed, it is plausible and supported by the actual observation that it stays a zero on one square metre. Preceding interpolation to annual recruitment rates per square metre (or minimum observed time intervals and plot areas) would therefore provide more realistic recruitment rates and reduce the discrepancies between unharmonized recruitment distributions. Further rescaling of recruitment rates would, for example, allow the application of beta regression techniques which can be extended, similar to discrete probability distributions, to zero-inflated distributions. Lastly, by eliminating sampling design factors, it would be possible to incorporate random effects into the model which could further improve model fits by eradicating regional misfits.

Lastly, this analysis serves as a proof of concept regarding the opportunities that arise by combining existing forest inventory data across large geographical ranges (code for the main analyses is available at https://github.com/loukoe/Tree-recruitment-analyses.git). Such datasets allow to further our understanding of forest dynamics and the development of more effective forest management strategies under climate change. Collecting such data sets requires great efforts, from the people who measure in the field, to the researchers who ensure the quality of the data, to those who use it for analysis and applications. This must be accompanied by long-term visions as acquiring forest inventories is yet a challenging endeavour (cf. Nabuurs et al., 2007, 2010). The data of more than 400,000 permanent sample plots that are currently measured by European countries (Lawrence et al., 2010) could

be made available, at least for research purposes. Further, countries could be encouraged to harmonise their NFI sampling strategies to reduce the challenges encountered through variations in plot area, size thresholds, and time intervals between the observations. In the context of forest regeneration, permanent measurements of trees below the diameter threshold may allow a better understanding of the detailed processes affecting tree recruitment. Today, most NFIs measure trees below the size threshold only temporarily.

5. Conclusions

Combining forest surveys to cover larger geographic ranges allows the detection and parameterisation of important climatic factors on tree recruitment. Our study revealed strong effects of climate on recruitment densities and species compositions. Recruitment success may experience a general decline under progressing climate change, with climatic variability, water limitations and temperature extremes as the main driver. Nevertheless, the results confirmed the major role of forest structure on forest regeneration that allows forest management to actively adapt to climate change. Nurturing mixed forests and measures that reduce drought impacts would promote higher tree recruitment densities and facilitate long-term benefits of resilient forest ecosystems. Lastly, effects of sampling strategies could not be eradicated entirely, and alternative modelling approaches should be explored with the aim to further reduce potential biases.

CRediT authorship contribution statement

Louis A. König: Writing – review & editing, Writing – original draft, Formal analysis, Data curation, Conceptualization. **Frits Mohren:** Writing – review & editing, Conceptualization. **Mart-Jan Schelhaas:** Writing – review & editing, Data curation, Conceptualization. **Julen Astigarraga:** Writing – review & editing, Data curation. **Emil Cienciala:** Writing – review & editing, Data curation. **Roman Flury:** Writing – review & editing, Methodology. **Jonas Fridman:** Writing – review & editing, Data curation. **Leen Govaere:** Writing – review & editing, Data curation. **Aleksi Lehtonen:** Writing – review & editing, Data curation. **Adriane E. Muelbert:** Writing – review & editing, Data curation. **Thomas A.M. Pugh:** Writing – review & editing, Data curation. **Brigitte Rohner:** Writing – review & editing, Data curation. **Paloma Ruiz-Benito:** Writing – review & editing, Data curation. **Susanne Suvanto:** Writing – review & editing, Data curation. **Andrzej Talarczyk:** Writing – review & editing, Data curation. **Miguel A. Zavala:** Writing – review & editing, Data curation. **Jose Medina Vega:** Writing – review & editing, Formal analysis. **Igor Staritsky:** Writing – review & editing, Data curation, Conceptualization. **Geerten Hengeveld:** Writing – review & editing, Data curation, Conceptualization. **Gert-Jan Nabuurs:** Writing – review & editing, Data curation, Conceptualization.

Declaration of competing interest

The authors declare that they have no known competing financial interests or personal relationships that could have appeared to influence the work reported in this paper.

Acknowledgements

Production Ecology & Resource Conservation (PE&RC) of Wageningen University. GJN and MJS acknowledge funding from the EU H2020 projects Verify (776810), HoliSoils (101000289), ForestPaths (101056755), Superb (101036849), Forwards (101084481), Resonate (101000574), and the Norwegian Research Council (NFR project 302701 Climate Smart Forestry Norway). JA was supported by a FPI fellowship of the Department of Education of the Basque Government. AL acknowledges funding from the Academy of Finland (grant agreement no. 325680, BiBiFe). EC acknowledges funding from the project AdAgriF—Advanced methods of greenhouse gases emission reduction and sequestration in agriculture and forest landscape for climate change mitigation (CZ.02.01.01/00/22_008/0004635). SS acknowledges funding from the European Union's Horizon 2020 research and innovation programme under the Marie Skłodowska-Curie grant agreement No 895158 (ForMMI). RF acknowledges the ETH Board in the framework of the Joint Initiative SCENE. The authors thank the two anonymous reviewers for their critical and yet constructive feedback that helped improving the manuscript. Lastly, the authors thank the numerous data providers and field crews of the nine forest inventories for their massive amount of work behind this database and for their supportiveness.

Supplementary materials

Supplementary material associated with this article can be found, in the online version, at doi:10.1016/j.ecolmodel.2025.111112.

Data availability

The authors do not have permission to share data. Code and processed data can be made available if the request includes permissions from all required data holders.

References

Adame, P., Rìo, M.d., Cañellas, I., 2010. Ingrowth model for pyrenean oak stands in north-western Spain using continuous forest inventory data. Eur. J. For. Res. 129 (4), 669–678. https://doi.org/10.1007/s10342-010-0368-1.

Allen, C.D., Macalady, A.K., Chenchouni, H., Bachelet, D., McDowell, N., Vennetier, M., Cobb, N., 2010. A global overview of drought and heat-induced tree mortality reveals emerging climate change risks for forests. For. Ecol. Manage. 259 (4), 660–684. https://doi.org/10.1016/j.foreco.2009.09.001.

Arlot, S., Celisse, A., 2010. A survey of cross-validation procedures for model selection. Stat. Surv. 4 (none), 40–79. https://doi.org/10.1214/09-SS054.

Beers, T.W., 1962. Components of forest growth. J. Forest. 60 (4), 245–248.

Binkley, D., Campoe, O.C., Gspaltl, M., Forrester, D.I., 2013. Light absorption and use efficiency in forests: why patterns differ for trees and stands. For. Ecol. Manage. 288, 5–13. https://doi.org/10.1016/j.foreco.2011.11.002.

Bogdziewicz, M., Crone, E.E., Steele, M.A., Zwolak, R., 2017. Effects of nitrogen deposition on reproduction in a masting tree: benefits of higher seed production are trumped by negative biotic interactions. J. Ecol. 105 (2), 310–320. https://doi.org/10.1111/1365-2745.12673.

Bolker, B.M., Brooks, M.E., Clark, C.J., Geange, S.W., Poulsen, J.R., Stevens, M.H.H., White, J.-S.S., 2009. Generalized linear mixed models: a practical guide for ecology and evolution. Trends Ecol. Evol. (Amst.) 24 (3), 127–135. https://doi.org/10.1016/j.tree.2008.10.008.

Bowyer, R.T., Bleich, V.C., Stewart, K.M., Whiting, J.C., Monteith, K.L., 2014. Density dependence in ungulates: a review of causes, and concepts with some clarifications. Calif. Fish Game 100 (3), 550–572. Retrieved from <Go to ISI>://WOS: 000350699500015.

Bravo, F., Pando, V., Ordonez, C., Lizarralde, I., 2008. Modelling ingrowth in mediterranean pine forests: a case study from scots pine (Pinus sylvestris L.) and mediterranean maritime pine (Pinus pinaster Ait.) stands in Spain. Investigacion Agraria-Sistemas Y Recursos Forestales 17 (3), 250–260. https://doi.org/10.5424/srf/2008173-01039.

Brooks, M.E., Kristensen, K., van Benthem, K.J., Magnusson, A., Berg, C.W., Nielsen, A., Bolker, B.M., 2017. glmmTMB Balances Speed and Flexibility Among Packages for Zero-inflated Generalized Linear Mixed Modeling. R J. 9 (2), 378–400. https://doi.org/10.32614/Rj-2017-066.

Bugmann, H., Seidl, R., 2022. The evolution, complexity and diversity of models of long-term forest dynamics. J. Ecol. 110 (10), 2288–2307. https://doi.org/10.1111/1365-2745.13989.

Bugmann, H., Seidl, R., Hartig, F., Bohn, F., Bruna, J., Cailleret, M., Reyer, C.P.O., 2019. Tree mortality submodels drive simulated long-term forest dynamics: assessing 15 models from the stand to global scale. Ecosphere 10 (2), e02616. https://doi.org/10.1002/ecs2.2616. ARTN.

Burkhart, H.E., Tome, M., 2012. Modeling Forest Trees and Stands. Springer Dordrecht Heidelberg New York London. https://doi.org/10.1007/978-90-481-3170-9.

Burnham, K.P., Anderson, D.R., 2002. Model Selection and Multimodel Inference: A practical Information-Theoretic Approach, 2nd ed. Springer Verlag.

Casper, B.B., Jackson, R.B., 1997. Plant competition underground. Annu. Rev. Ecol. Syst. 28, 545–570. https://doi.org/10.1146/annurev.ecolsys.28.1.545.

Catovsky, S., Bazzaz, F.A., 2002. Nitrogen availability influences regeneration of temperate tree species in the understory seedling bank. Ecol. Appl. 12 (4), 1056–1070. https://doi.org/10.2307/3061036.

Catovsky, S., Kobe, R.K., Bazzaz, F.A., 2002. Nitrogen-induced changes in seedling regeneration and dynamics of mixed conifer–broad-leaved forests. Ecol. Appl. 12 (6), 1611–1625. https://doi.org/10.1890/1051-0761(2002)012[1611:NICISR]2.0.CO;2.

Cienciala, E., Russ, R., Šantrůčková, H., Altman, J., Kopáček, J., Hůnová, I., Ståhl, G., 2016. Discerning environmental factors affecting current tree growth in Central Europe. Sci. Total Environ. 573, 541–554. https://doi.org/10.1016/j.scitotenv.2016.08.115.

Dalsgaard, L., 2007. Above and below ground gaps: the effects of a small canopy opening on throughfall, soil moisture and tree transpiration in Suserup Skov, Denmark. Ecol. Bull. (52), 81–102. Retrieved from http://www.jstor.org/stable/20113341.

Eerikäinen, K., Valkonen, S., Saksa, T., 2014. Ingrowth, survival and height growth of small trees in uneven-aged Picea abies stands in southern Finland. Forest Ecosyst. 1 (1), 5. https://doi.org/10.1186/2197-5620-1-5.

EMEP (2021). Co-operative programme for monitoring and evaluation of the long-range transmission of air pollutants in Europe. Retrieved from https://www.emep.int/.

Esquivel-Muelbert. (in prep.). Remarkable disequilibrium across Earth's forests.

EUROPE, F. (2020). State of Europe's Forests 2020. Retrieved from.

Feldmann, E., Glatthorn, J., Hauck, M., Leuschner, C., 2018. A novel empirical approach for determining the extension of forest development stages in temperate old-growth forests. Eur. J. For. Res. 137 (3), 321–335. https://doi.org/10.1007/s10342-018-1105-4.

Feng, C., 2022. Zero-inflated models for adjusting varying exposures: A cautionary note on the pitfalls of using offset. J. Appl. Stat. 49 (1), 1–23. https://doi.org/10.1080/02664763.2020.1796943.

Flury, R., Portier, J., Rohner, B., Baltensweiler, A., Di Bella Meusburger, K., Scherrer, D., Thürig, E., Stadelmann, G., 2024. Soil and climate-dependent ingrowth inference: broadleaves on their slow way to conquer Swiss forests. Ecography. 2024 (7), e07174. https://doi.org/10.1111/ecog.07174.

Fortin, M., DeBlois, J., 2007. Modeling tree recruitment with zero-inflated models: the example of hardwood stands in southern Quebec, Canada. Forest Sci. 53 (4), 529–539. Retrieved from <Go to ISI>://WOS:000248642500008.

Forzieri, G., Girardello, M., Ceccherini, G., Spinoni, J., Feyen, L., Hartmann, H., Cescatti, A., 2021. Emergent vulnerability to climate-driven disturbances in European forests. Nat. Commun. 12 (1), 1081. https://doi.org/10.1038/s41467-021-21399-7. ARTN.

Gilbert, B., Lechowicz, M.J., 2004. Neutrality, niches, and dispersal in a temperate forest understory. Proc. Natl Acad. Sci. 101 (20), 7651–7656. https://doi.org/10.1073/pnas.0400814101.

Glatthorn, J., Feldmann, E., Tabaku, V., Leuschner, C., Meyer, P., 2018. Classifying development stages of primeval European beech forests: is clustering a useful tool? BMC Ecol. 18, 47. https://doi.org/10.1186/s12898-018-0203-y. ARTN.

Graumlich, L.J., 1991. Subalpine tree growth, climate, and increasing CO_2: an assessment of recent growth trends. Ecology. 72 (1), 1–11. https://doi.org/10.2307/1938895.

Harvey, J.E., Smiljanic, M., Scharnweber, T., Buras, A., Cedro, A., Cruz-Garcia, R., Wilmking, M., 2020. Tree growth influenced by warming winter climate and summer moisture availability in northern temperate forests. Glob. Chang. Biol. 26 (4), 2505–2518. https://doi.org/10.1111/gcb.14966.

Hartig, F., 2024. DHARMa: residual Diagnostics for Hierarchical (Multi-Level /Mixed) Regression Model (Version R package version 0.4.7, <. https://CRAN.R-project.org/package=DHARMa. >).

Hasenauer, H., 2006. Sustainable forest management: growth models for Europe. Springer Berlin Heidelberg. https://doi.org/10.1007/3-540-31304-4.

Hengl, T., de Jesus, J.M., MacMillan, R.A., Batjes, N.H., Heuvelink, G.B.M., Ribeiro, E., Gonzalez, M.R., 2014. SoilGrids1km-global soil information based on automated mapping. PLoS. One 9 (8), e105992. https://doi.org/10.1371/journal.pone.0105992. ARTN.

Hijmans, R.J., Cameron, S.E., Parra, J.L., Jones, P.G., Jarvis, A., 2005. Very high resolution interpolated climate surfaces for global land areas. Int. J. Climatol. 25 (15), 1965–1978. https://doi.org/10.1002/joc.1276.

Hülsmann, L., Bugmann, H., Brang, P., 2017. How to predict tree death from inventory data — lessons from a systematic assessment of European tree mortality models. Canad. J. Forest Res. 47 (7), 890–900. https://doi.org/10.1139/cjfr-2016-0224.

Ibanez, I., Clark, J.S., LaDeau, S., HilleRisLambers, J., 2007. Exploiting temporal variability to understand tree recruitment response to climate change. Ecol. Monogr. 77 (2), 163–177. https://doi.org/10.1890/06-1097.

Iida, S., Masaki, T., 2002. Seed Dynamics. In: Nakashizuka, T., Matsumoto, Y. (Eds.), Diversity and Interaction in a Temperate Forest Community: Ogawa Forest Reserve of Japan. Springer Japan, Tokyo, pp. 127–141.

Jabro, J.D., Evans, R.G., Kim, Y., Iversen, W.M., 2009. Estimating in situ soil-water retention and field water capacity in two contrasting soil textures. Irrigat. Sci. 27 (3), 223–229. https://doi.org/10.1007/s00271-008-0137-9.

JRC, 2021. Joint Research Centre: agri4Cast ToolBox. Retrieved from. https://agri4cast.jrc.ec.europa.eu/. h t tps://agri4cast.jrc.ec.europa.eu/.

Käber, Y., Meyer, P., Stillhard, J., De Lombaerde, E., Zell, J., Stadelmann, G., Bigler, C., 2021. Tree recruitment is determined by stand structure and shade tolerance with

uncertain role of climate and water relations. Ecol. Evol. 11 (17), 12182–12203. https://doi.org/10.1002/ece3.7984.

Kara, F., Topacoglu, O., 2018. Influence of stand density and canopy structure on the germination and growth of Scots pine (Pinus sylvestris L.) seedlings. Environ. Monit. Assess. 190 (12), 749. https://doi.org/10.1007/s10661-018-7129-x. ARTN.

Klopcic, M., Poljanec, A., Boncina, A., 2012. Modelling natural recruitment of European beech (Fagus sylvatica L.). For. Ecol. Manage. 284, 142–151. https://doi.org/10.1016/j.foreco.2012.07.049.

Koenig, W.D., Knops, J.M.H., 2000. Patterns of annual seed production by Northern hemisphere trees: a global perspective. Am. Nat. 155 (1), 59–69. https://doi.org/10.1086/303302.

König, A.L., Mohren, F., Schelhaas, M.J., Bugmann, H., Nabuurs, G.J., 2022. Tree regeneration in models of forest dynamics-Suitability to assess climate change impacts on European forests. For. Ecol. Manage. 520, 120390. https://doi.org/10.1016/j.foreco.2022.120390. ARTN.

Kunz, J., Löffler, G., Bauhus, J., 2018. Minor European broadleaved tree species are more drought-tolerant than Fagus sylvatica but not more tolerant than Quercus petraea. For. Ecol. Manage. 414, 15–27. https://doi.org/10.1016/j.foreco.2018.02.016.

Lawrence, M., McRoberts, R.E., Tomppo, E., Gschwantner, T., Gabler, K., 2010. Comparisons of National Forest Inventories. In: Tomppo, E., Gschwantner, T., Lawrence, M., McRoberts, R.E. (Eds.), *National Forest Inventories: Pathways for Common Reporting*. Springer, Netherlands, pp. 19–32. https://doi.org/10.1007/978-90-481-3233-1_2.

Ledermann, T., 2002. Estimating Ingrowth (Tree Recruitment) using Data from the Austrian National Forest Inventory 1981-1996. Austr. J. Forest Sci. 119, 40–76.

Lerink, B.J.W., Schelhaas, M.-J., Schreiber, R., Aurenhammer, P., Kies, U., Vuillermoz, M., Nabuurs, G.-J., 2023. How much wood can we expect from European forests in the near future? For. Int. J. Forest Res. cpad009. https://doi.org/10.1093/forestry/cpad009.

Lévesque, M., Saurer, M., Siegwolf, R., Eilmann, B., Brang, P., Bugmann, H., Rigling, A., 2013. Drought response of five conifer species under contrasting water availability suggests high vulnerability of Norway spruce and European larch. Glob. Chang. Biol. 19 (10), 3184–3199. https://doi.org/10.1111/gcb.12268.

Li, R.X., Weiskittel, A.R., Kershaw, J.A., 2011. Modeling annualized occurrence, frequency, and composition of ingrowth using mixed-effects zero-inflated models and permanent plots in the Acadian Forest Region of North America. Canad. J. Forest Res. 41 (10), 2077–2089. https://doi.org/10.1139/X11-117.

Mäkipää, R., Heikkinen, J., 2003. Large-scale changes in abundance of terricolous bryophytes and macrolichens in Finland. J. Veget. Sci. 14 (4), 497–508. https://doi.org/10.1111/j.1654-1103.2003.tb02176.x.

Marryanna, L., Noguchi, S., Kosugi, Y., Niiyama, K., Itoh, M., Sato, T., Abd-Rahman, K., 2019. Spatial distribution of soil moisture and its influence on stand structure in a lowland Dipterocarp Forest in Peninsular Malaysia. J. Trop. Forest Sci. 31 (2), 135–150. https://doi.org/10.26525/jtfs2019.31.2.135150.

Mason, W.L., Diaci, J., Carvalho, J., Valkonen, S., 2022. Continuous cover forestry in Europe: usage and the knowledge gaps and challenges to wider adoption, 2021 Forestry 95, 1. https://doi.org/10.1093/forestry/cpac008.

McCann, K.S., 2000. The diversity–stability debate. Nature 405 (6783), 228–233. https://doi.org/10.1038/35012234.

Metzger, J.C., Wutzler, T., Dalla Valle, N., Filipzik, J., Grauer, C., Lehmann, R., Hildebrandt, A., 2017. Vegetation impacts soil water content patterns by shaping canopy water fluxes and soil properties. Hydrol. Process. 31 (22), 3783–3795. https://doi.org/10.1002/hyp.11274.

Metzger, M.J., Bunce, R.G.H., Jongman, R.H.G., Sayre, R., Trabucco, A., Zomer, R., 2013. A high-resolution bioclimate map of the world: a unifying framework for global biodiversity research and monitoring. Glob. Ecol. Biogeogr. 22 (5), 630–638. https://doi.org/10.1111/geb.12022.

Moon, G.H., Yim, J.S., Moon, N.H., Shin, M.Y., 2019. Development of ingrowth models for forest types in South Korea. Forest. Sci. Technol. 15 (4), 221–229. https://doi.org/10.1080/21580103.2019.1671904.

Mugasha, W.A., Eid, T., Bollandsås, O.M., Mbwambo, L., 2017. Modelling diameter growth, mortality and recruitment of trees in miombo woodlands of Tanzania. Southern For. J. Forest Sci. 79 (1), 51–64. https://doi.org/10.2989/20702620.2016.1233755.

Müller-Haubold, H., Hertel, D., Leuschner, C., 2015. Climatic drivers of mast fruiting in European Beech and resulting C and N allocation shifts. Ecosystems. 18 (6), 1083–1100. https://doi.org/10.1007/s10021-015-9885-6.

Nabuurs, G.J., Hengeveld, G.M., van der Werf, D.C., Heidema, A.H., 2010. European forest carbon balance assessed with inventory based methods—An introduction to a special section. For. Ecol. Manage. 260 (3), 239–240. https://doi.org/10.1016/j.foreco.2009.11.024.

Nabuurs, G.J., van der Werf, D.C., Heidema, A.H., van den Wyngaert, I.J.J., 2007. Towards a high resolution forest carbon balance for Europe based on inventory data. CABI 105–111. https://doi.org/10.1079/9781845932947.0105.

Neumann, M., Mues, V., Moreno, A., Hasenauer, H., Seidl, R., 2017. Climate variability drives recent tree mortality in Europe. Glob. Chang. Biol. 23 (11), 4788–4797. https://doi.org/10.1111/gcb.13724.

Newland, M.C., 2019. An information theoretic approach to model selection: a tutorial with Monte Carlo confirmation. Persp. Behav. Sci. 42 (3), 583–616. https://doi.org/10.1007/s40614-019-00206-1.

Pham, V.V., Ammer, C., Annighofer, P., Heinrichs, S., 2022. Tree regeneration characteristics in limestone forests of the Cat Ba National Park, Vietnam. Bmc Ecol. Evol. 22 (1), 6. https://doi.org/10.1186/s12862-021-01957-9. ARTN.

Pretzsch, H., 2009. Forest dynamics, growth and yield. From measurement to model. Springer-Verlag Berlin Heidelberg. https://doi.org/10.1007/978-3-540-88307-4.

Pretzsch, H., Biber, P., 2005. A re-evaluation of Reineke's rule and stand density index. Forest Sci. 51 (4), 304–320. Retrieved from <Go to ISI>://WOS:000231006800004.

Price, D.T., Zimmermann, N.E., van der Meer, P.J., Lexer, M.J., Leadley, P., Jorritsma, I. T.M., Smith, B., 2001. Regeneration in gap models: priority issues for studying forest responses to climate change. Clim. Change 51 (3–4), 475–508. https://doi.org/10.1023/A:1012579107129.

Proll, G., Dullinger, S., Dirnbock, T., Kaiser, C., Richter, A., 2011. Effects of nitrogen on tree recruitment in a temperate montane forest as analysed by measured variables and Ellenberg indicator values. Preslia 83 (1), 111–127. Retrieved from <Go to ISI>://WOS:000289502000005.

Rohner, B., Waldner, P., Lischke, H., Ferretti, M., Thurig, E., 2018. Predicting individual-tree growth of central European tree species as a function of site, stand, management, nutrient, and climate effects. Eur. J. For. Res. 137 (1), 29–44. https://doi.org/10.1007/s10342-017-1087-7.

Schelhaas, M.-J., Hengeveld, G.M., Heidema, N., Thürig, E., Rohner, B., Vacchiano, G., Nabuurs, G.-J., 2018a. Species-specific, pan-European diameter increment models based on data of 2.3 million trees. For. Ecosyst. 5 (1), 21. https://doi.org/10.1186/s40663-018-0133-3.

Schelhaas, M.J., Hengeveld, G.M., Heidema, N., Thurig, E., Rohner, B., Vacchiano, G., Nabuurs, G.J., 2018c. Species-specific, pan-European diameter increment models based on data of 2.3 million trees. For. Ecosyst. 5. https://doi.org/10.1186/s40663-018-0133-3. ARTN 21.

Shifley, S.R., Ek, A.R., Burk, T.E., 1993. A generalized methodology for estimating forest ingrowth at multiple threshold diameters. Forest Sci. 39 (4), 776–798. https://doi.org/10.1093/forestscience/39.4.776.

Shugart, H.H., 1984. A Theory of Forest Dynamics. Springer-Verlag, New York.

St George, S., Meko, D.M., Cook, E.R., 2010. The seasonality of precipitation signals embedded within the North American Drought Atlas. Holocene 20 (6), 983–988. https://doi.org/10.1177/0959683610365937.

Team, R.C., 2022. R: A language and Environment For Statistical Computing. R Foundation for Statistical Computing, Vienna, Austria. Retrieved from. https://www.R-project.org/.

Thrippleton, T., Bugmann, H., Snell, R.S., 2018. Herbaceous competition and browsing may induce arrested succession in central European forests. J. Ecol. 106 (3), 1120–1132. https://doi.org/10.1111/1365-2745.12889.

Tiebel, K., Huth, F., Wagner, S., 2018. Soil seed banks of pioneer tree species in European temperate forests: a review. [Soil seed banks of pioneer tree species in European temperate forests: a review]. iForest - Biogeosci. For. 11 (1), 48–57. https://doi.org/10.3832/ifor2400-011.

Tomppo, E., Gschwantner, L.M., McRoberts, R. (2010). *National forest inventories: pathways for common reporting.*.

Trabucco, A., Zomer, R.J., Bossio, D.A., van Straaten, O., Verchot, L.V., 2008. Climate change mitigation through afforestation/reforestation: a global analysis of hydrologic impacts with four case studies. Agric. Ecosyst. Environ. 126 (1–2), 81–97. https://doi.org/10.1016/j.agee.2008.01.015.

van der Waal, C., de Kroon, H., de Boer, W.F., Heitkonig, I.M.A., Skidmore, A.K., de Knegt, H.J., Prins, H.H.T., 2009. Water and nutrients alter herbaceous competitive effects on tree seedlings in a semi-arid savanna. J. Ecol. 97 (3), 430–439. https://doi.org/10.1111/j.1365-2745.2009.01498.x.

Vanclay, J.K., 1994. Modelling Forest Growth and yield: Applications to Mixed Tropical forests; Chapter 10: Regeneration and Recruitment. CAB International, pp. 192–203.

Vanclay, J.K., 2014. Forest Growth and Yield Modeling. Wiley StatsRef: Statistics Reference Online.

Venables, W.N., Ripley, B.D., 2002. Modern Applied Statistics With S. Fourth Edition. Springer, New York.

Weiskittel, A.R., Hann, D.W., Kershaw, J.A., Vanclay, J.K., 2011. Forest Growth and Yield Modeling. John Wiley & Sons, Ltd. https://doi.org/10.1002/9781119998518.

Willson, K.G., Cox, L.E., Hart, J.L., Dey, D.C., 2020. Three-dimensional light structure of an upland Quercus stand post-tornado disturbance. J. For. Res. 31 (1), 141–153. https://doi.org/10.1007/s11676-019-00907-y.

Yan, Y., Zhang, C., Wang, Y., Zhao, X., von Gadow, K., 2015. Drivers of seedling survival in a temperate forest and their relative importance at three stages of succession. Ecol. Evol. 5 (19), 4287–4299. https://doi.org/10.1002/ece3.1688.

Yang, Y., Huang, S., 2015. Two-stage ingrowth models for four major tree species in Alberta. Eur. J. For. Res. 134, 991–1004.

Zell, J., Rohner, B., Thurig, E., Stadelmann, G., 2019. Modeling ingrowth for empirical forest prediction systems. For. Ecol. Manage. 433, 771–779. https://doi.org/10.1016/j.foreco.2018.11.052.

Zhang, X.Q., Lei, Y.C., Cai, D.X., Liu, F.Q., 2012. Predicting tree recruitment with negative binomial mixture models. For. Ecol. Manage. 270, 209–215. https://doi.org/10.1016/j.foreco.2012.01.028.

Zorner, R.J., Trabucco, A., Bossio, D.A., Verchot, L.V., 2008. Climate change mitigation: a spatial analysis of global land suitability for clean development mechanism afforestation and reforestation. Agric. Ecosyst. Environ. 126 (1–2), 67–80. https://doi.org/10.1016/j.agee.2008.01.014.

Zuur, A.F., A, A, S., Ieno, E.N., 2012. Zero Inflated Models and Generalized Linear Mixed Models With R. Highland Statistics Ltd, Newburgh.

Zuur, A.F., Ieno, E.N., Elphick, C.S., 2010. A protocol for data exploration to avoid common statistical problems. Methods Ecol. Evol. 1 (1), 3–14. https://doi.org/10.1111/j.2041-210X.2009.00001.x.